

Contrast-enhanced computed tomography combined with Chitosan-Fe₃O₄ nanoparticles targeting fibroblast growth factor receptor and vascular endothelial growth factor receptor in the screening of early esophageal cancer

JUANJUAN GAI^{1*}, ZHENLI GAO^{1*}, LIQIANG SONG², YONGYUN XU³, WEIXIN LIU² and CHUANXIN ZHAO⁴

Departments of ¹Radiology, ²Oncology, ³Computed Tomography and ⁴Joint Surgery, Dongying People's Hospital, Dongying, Shandong 257091, P.R. China

Received November 17, 2016; Accepted April 28, 2017

DOI: 10.3892/etm.2018.6087

Abstract. Esophageal cancer is a malignant tumor with a relatively high invasiveness, metastatic potential and worldwide incidence among human cancers. The majority of patients with esophageal cancer are diagnosed in a late tumor stage due to a lack of advanced and sensitive protocols for the diagnosis of patients with early-stage esophageal cancer. In the current study, contrast-enhanced computerized tomography (CECT) combined with Chitosan-Fe₃O₄ nanoparticles targeting fibroblast growth factor receptor (FGFR) and vascular endothelial growth factor receptor (VEGFR; CECT-CNFV) were used to diagnose patients with suspected esophageal cancer. A Chitosan-Fe₃O₄-parceled bispecific antibody targeting FGFR and VEGFR was produced and its affinity to esophageal cancer cells was determined both *in vitro* and *in vivo*. A total of 320 patients with suspected esophageal cancer were voluntarily recruited to evaluate the efficacy of CECT-CNFV in the diagnosis of early-stage esophageal cancer. All participants were subjected to CT and CECT-CNFV to detect whether tumors were present in the esophageal area. A Chitosan-Fe₃O₄ nanoparticles contrast agent was orally administered at 20 min prior to CT and CECT-CNFV. The results demonstrated that CECT-CNFV improved diagnostic sensitivity and provided a novel protocol for the diagnosis of tumors in patients with suspected gastric cancer at an early-stage. Furthermore, the resolution ratio of images was enhanced by CECT-CNFV, which enabled the visualization of tiny tumor nodules in esophageal tissue. Clinical data demonstrated

that CECT-CNFV diagnosed 200 patients with suspected early-stage esophageal cancer and 120 patients as tumor free. In addition, CECT-CNFV exhibited higher signal enhancement of tumor nodules than CT, suggesting a higher accuracy and accumulation of nanoparticle contrast agent within the tumor nodules of esophageal tissue. Notably, the survival rate of patients with esophageal cancer diagnosed at an early-stage by CECT-CNFV was higher than the mean five-year survival rate ($P < 0.01$). In conclusion, CECT-CNFV enhanced the sensitivity and accuracy of CT in the diagnosis of early-stage esophageal cancer. Thus, CECT-CNFV may improve the accuracy of CT in the diagnosis of mural enhancement in patients with esophageal cancer.

Introduction

Esophageal cancer is the most common malignant tumor of the digestive tract (1). Clinical data has demonstrated that, worldwide, ~300,000 cases of esophageal cancer result in mortality each year (2,3). A previous systematic review and meta-analysis evaluated the health-related quality of life of patients with esophageal cancer following potentially curative treatment and results identified that health-related quality of life of patients with esophageal cancer is an indicator to evaluate the efficacy of anti-cancer drugs (4). Although increasing cancer therapy technologies continue to be investigated in clinical studies, the five-year survival rate of patients with esophageal cancer is lower than 12.5% (5). Previous reports have indicated that C-X-C motif chemokines, their cognate receptors and tumor metastasis-associated proteins are involved in the pathogenesis of human esophageal cancer (6,7). In addition, lymph node, lung and stomach metastases are key prognostic indicators in late-stage esophageal cancer, with metastatic tumor cell expansion leading to a shortened survival rate (8-10). Therefore, the prevention and early diagnosis of esophageal cancer may enhance the cure rate and improve survival in patients with early-stage esophageal cancer.

Currently, the majority of patients clinically diagnosed with esophageal cancer are in an advanced stage of the disease (11). Although a number of reports have introduced various diagnostic techniques for early-stage esophageal

Correspondence to: Professor Liqiang Song, Department of Oncology, Dongying People's Hospital, 317 Dongcheng South Road, Dongying, Shandong 257091, P.R. China
E-mail: songliqiangprof@163.com

*Contributed equally

Key words: esophageal cancer, Chitosan-Fe₃O₄, CECT-CNFV, early diagnosis

cancer, including Raman spectroscopy, chemometric techniques, image-enhanced magnifying endoscopy, endoscopic ultrasound elastography and contrast-enhanced computerized tomography (CECT), CECT is the most frequently used method for the diagnosis of esophageal cancer and lymph node metastasis (12-14). Although CECT is considered to have many advantages, its relatively low resolution makes it inconclusive in the final diagnosis of patients with suspected cancer (15,16). Due to the lack of data on early-stage cancer, comprehensive treatments and effective therapeutic plans have not been developed for patients with suspected early-stage cancer (17,18).

Clinically, contrast agent improves the resolution of CT, and the most commonly used contrast agents are employed during ultrasound examination, due to their resonance following exposure to ultrasound waves (19,20). Previous results have indicated that contrast agent combined with CT may be used for the diagnosis of tumor stage and progression (21). More recently, nanoscale microbubbles of contrast agents have been developed and clinically applied in disease diagnosis (22). Therefore, nanoscale microbubbles specific to the tumor markers of esophageal cancer may improve the diagnostic sensitivity and resolution of CT in the diagnosis of patients with early-stage or suspected esophageal cancer.

Previous reports have suggested that fibroblast growth factor receptor (FGFR) is overexpressed in tumor cells, and tumor vasculature may be regulated by FGF/FGFR signaling-mediated angiogenesis and bone marrow-derived cell recruitment (23,24). Previous results have also indicated that vascular endothelial growth factor receptor (VEGFR) is overexpressed and associated with tumor growth, aggressiveness and tumor angiogenesis in the progression of human cancers (25,26). In the present study, the efficacy of CECT combined with nanoscale microbubble contrast agent targeting of FGFR and VEGFR was investigated in patients with suspected esophageal cancer. Results of this clinical analysis demonstrated the potential applications of CECT combined with Chitosan-Fe₃O₄ nanoparticles targeting FGFR and VEGFR (CECT-CNFV) for improving imaging modality and diagnostic sensitivity in the diagnosis of esophageal cancer. The present outcomes indicated that CECT-CNFV improved image resolution and diagnostic accuracy for the early diagnosis and final confirmation of suspected cases, suggesting that CECT-CNFV may be a potential diagnostic method for early-stage esophageal cancer.

Materials and methods

Ethics statement. The present clinical design (approval number: DPHSP20080124M) was carried out in accordance with the recommendations in the Guide for the Care and Use of Clinical Study of the Pharmaceutical Administration Law of China (27). The present study was approved by the Ethics Committee of Dongying People's Hospital (Dongying, China). All clinical examination and testing procedures were performed according to standard operating procedures, and all patients provided written informed consent.

Patients and volunteers. A total of 320 patients with suspected esophageal cancer aged 24.3-75.4 years old from Dongying

People's Hospital (Dongying, China) were enrolled in the present study between May 2014 and January 2016. Among these patients, 156 were male and 164 were female. Control tissues and cells were obtained from 6 patients (3 male and 3 female) who were diagnosed as tumor free. The mean age of control patients was 42.5 years old. All patients were subjected to CECT and CECT-CNFV for the detection of early-stage esophageal cancer. The characteristics of patients with suspected esophageal cancer are summarized in Table I. After diagnosis by CECT and CECT-CNFV, patient survival was investigated in a 60-month long-term observation period. All patients were investigated and patients were assessed every two months.

Nanoparticles contrast agent. Novel Chitosan-Fe₃O₄ nanoparticles encapsulated by bispecific antibody against FGFR and VEGFR (BisFV) were used as a CNFV contrast agent to improve the imaging resolution ratio and diagnostic sensitivity of early-stage esophageal cancer diagnosis. BisFV antibody was a gift from Professor Yuan Hui of the Biological Pharmaceutical Laboratory at Shandong University of Science and Technology (Qingdao, China) Chitosan-Fe₃O₄-encapsulated BisFV was manufactured according to the covalent bonding method described in a previous study (28). The CNFV contrast agent (1-10 mg/kg, n=10; 10-25 mg/kg, n=14; 25-40 mg/kg, n=18) was orally taken at 20 min prior to CECT-CNFV to allow adherence to esophageal cancer cells. Following the 20 min pretreatment, CNFV was visualized using a CECT system. The signal intensity was analyzed using CECT system.

Pharmacodynamics of BisFV. Plasma concentration of BisFV was analyzed in patients with suspected esophageal cancer following treatment with CNFV contrast agent. Blood samples were collected from 32 participants at 0, 6, 12, 18 and 24 h following administration of CNFV contrast agent. Plasma BisFV levels were determined using liquid chromatography-tandem mass spectrometry as described previously (29).

Scan protocol. A 64-multidetector CECT diagnosis system (Philips Medical Systems, Inc., Bothell, WA, USA) was used to measure the efficacy of CNFV using a preprogrammed setting. The preprogrammed setting was optimized to record the best image formation. The esophagus of all patients was scanned by CECT, according to the instructions of the CECT system. The parameters and settings of CECT were as described in a previous study (30). CECT and CECT-CNFV imaging was performed in all patients with suspected esophageal cancer.

Image data analysis. Data from the CECT-CNFV and CECT image sets were analyzed using a CT system (Version 2.3, Shimadzu, Kyoto, Japan). Esophageal cancer masses were detected in the CECT or CECT-CNFV images. The patients with suspected early-stage gastric cancer were analyzed CECT-CNFV. The sizes of tumor nodules were evaluated in regions of stomach tumor lesions using the CT system.

Treatment of esophageal cancer patients diagnosed by CECT-CNFV. Following diagnosis of early-stage esophageal cancer using CECT-CNFV, patients immediately received different treatments following diagnosis, including

radiotherapy, chemotherapy, Chinese medicine, biological therapy and comprehensive therapy (Table II). The median overall survival and median progression-free survival of patients with esophageal cancer were analyzed according to a previously described method (31).

Western blot analysis. Western blot analysis was performed as previously described (32). Tumor cells were lysed in lysate buffer containing protease-inhibitor (cat no. P3480, Sigma-Aldrich; Merck KGaA) and were centrifuged at 8,000 x g at 4°C for 10 min. Protein concentration was measured using a BCA protein assay kit. Protein samples (20 µg) were resolved using 15% SDS-PAGE and then transferred to polyvinylidene fluoride membranes (Merck KGaA). After 1 h blocking at 37°C using 10% blocking reagent (Roche Applied Science, Penzberg, Germany), membranes were incubated with primary antibodies: mouse anti-human FGFR (1:1,000, cat no. ab10646), mouse anti-human VEGFR (1:1,000, cat no. ab2349) and β-actin (1:1,000, cat no. ab124721, all Abcam, Cambridge, UK) for 12 h at 4°C. Membranes were then washed three times in TBST and incubated with HRP-conjugated Immunoglobulin G mAb (1:2,000; cat no. PV-6001; ZSGB-BIO, Beijing, China) for 1 h at 37°C. Following three washed in TBST, membranes were developed using a chemiluminescence assay system (Roche) and exposed on Kodak exposure films. Densitometric quantification of the immunoblot data was performed using the software of Quantity-One (Bio-Rad Laboratories, Hercules, CA, USA).

ELISA. Serum levels of FGFR (cat no. DYC766-2, Bio-Rad Laboratories), VEGFR (cat no. DYC1780-2, Bio-Rad Laboratories) were detected using ELISA kits according to the manufacturer's protocol. Serum concentration levels of FGFR and VEGFR were measured using enzyme micro-plate reader at a wavelength of 450 nm.

Immunofluorescence staining. After esophageal cancer was confirmed in patients by CECT-CNFV, esophageal tumor cells isolated from patients on day 7 using tumor resection were cultured in minimum essential medium (Gibco; Thermo Fisher Scientific, Inc., Waltham, MA, USA) supplemented with 10% heat-inactivated fetal bovine serum (Gibco; Thermo Fisher Scientific, Inc.) *in vitro*. Esophageal tumor cells were incubated with mouse anti-human FGFR (1:1,000, cat no. ab10646, Abcam, Cambridge UK) or mouse anti-human VEGFR (1:1,000, cat no. ab2349, Abcam) for 2 h at 37°C, then washed three times with phosphate-buffered saline. Cells were incubated with red fluorescence-labeled goat anti-mouse (1:1,000, cat no. ab150117, Abcam) or red fluorescence-labeled (1:1,000, cat no. ab150115, Abcam) goat anti-mouse IgG for 30 min at 37°C. Esophageal tumor cells were observed under a fluorescence microscope. The immunofluorescence procedures have previously been reported in detail (33).

Immunohistochemistry. Esophageal tumors and normal esophageal tissues (tumor free individuals) from patients were fixed with 10% formaldehyde for 2 h at 37°C, then embedded in paraffin and cut into tumor 4 µm thick sections. Antigen retrieval was performed on the tumor sections

Table I. Characteristics of patients with esophageal cancer.

Characteristic	Male	Female
Number, n	156	164
Age, range	24.3-66.6	26.3-75.4
Medical history of cancer	2	3
Blood pressure (mm Hg)	108.4±17.2	103.5±16.1
Blood glucose (mmol/l)	7.2±3.7	8.2±3.2
Diagnostic method		
CECT	156	164
CECT-CNFV	156	164

CECT, contrast-enhanced computed tomography; CECT-CNFV, CECT combined with Chitosan-Fe₃O₄ nanoparticles targeting fibroblast growth factor receptor and vascular endothelial growth factor receptor.

Table II. Treatment of patients with esophageal cancer diagnosed by contrast-enhanced computed tomography combined with Chitosan-Fe₃O₄ nanoparticles targeting fibroblast growth factor receptor and vascular endothelial growth factor receptor.

Variable	Male	Female
Number, n	56	64
Treatment		
Radiotherapy	12	16
Chemotherapy	14	12
Chinese medicine	15	18
Biological therapy	15	18
Comprehensive therapy	34	45

Table III. Confirmation of contrast agent nanoparticle dosage for patients with esophageal cancer.

Variable	Dosage, mg/kg		
	1-10 (n=10)	10-25 (n=14)	25-40 (n=18)
Signal intensity (HU)	56.2±8.8	86.7±10.3	83.5±12.5
Sensitivity (%)	65.6±12.2	81.2±12.6	82.6±11.6

using eBioscience™ IHC Antigen Retrieval Solution (cat no. 00-4955-58, Invitrogen; Thermo Fisher Scientific, Inc.), sections were washed with PBST (Sigma-Aldrich; Merck KGaA) and subsequently incubated with mouse anti-human FGFR (1:1,000, cat no. ab10646, Abcam) or mouse anti-human VEGFR antibodies (1:1,000, cat no. ab2349, Abcam) for 12 h at 4°C. Following antibody incubation, proteins were washed with PBST three times and incubated with Alexa Fluor 488-labeled secondary antibodies (1:500; Beyotime Institute of Biotechnology, Haimen, China) for 2 h at 37°C and the

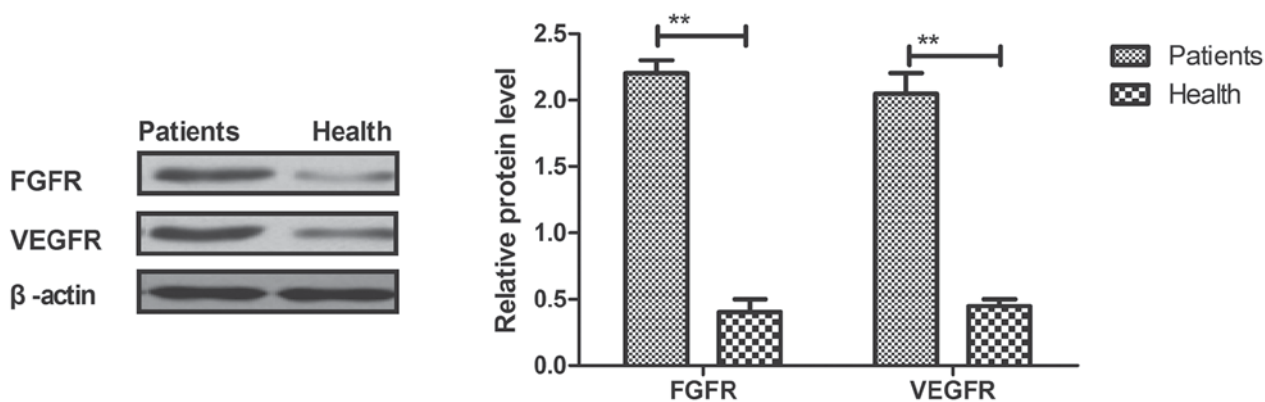


Figure 1. Comparison of FGFR and VEGFR expression between esophageal cancer patients and healthy volunteers. A Student's t test revealed a significant effect. ** $P < 0.01$ vs. health. FGFR, fibroblast growth factor receptor; VEGFR, vascular endothelial growth factor receptor.

specimens were visualized. A Diaminobenzidine staining system (D7679MSDS, Sigma-Aldrich; Merck KGaA) was used to detect target protein expression according to manufacturer's protocol. For histological staining, tumor sections were stained with hematoxylin and eosin and observed using a light microscope (Olympus BX51, Olympus Corporation, Tokyo, Japan) as described previously (34).

Statistical analysis. Data were presented as the mean \pm standard deviation of triplicate experiments. All data were analyzed using SPSS Statistics 19.0 (IBM Corp., Armonk, NY, USA). Unpaired data were analyzed using a Student's t test and comparisons between the data of multiple groups were performed using one-way analysis of variance followed by Dunnett's t test. $P < 0.05$ was considered to indicate a statistically significant difference. Kaplan-Meier analysis was used to estimate the survival rate of patients from a 60-month long-term observation.

Results

FGFR and VEGFR expression in the tumor cells of esophageal cancer patients. The expressions of FGFR and VEGFR in the tumor cells of patients with esophageal cancer were assessed. As depicted in Figs. 1 and 2, the expression and plasma levels of FGFR and VEGFR were upregulated in the tumor cells of esophageal cancer patients when compared with normal esophageal cells ($P < 0.01$). Immunohistochemistry also indicated that FGFR and VEGFR were upregulated in clinical esophageal tumor tissues when compared with normal esophageal tissues (Fig. 3). Furthermore, immunofluorescence demonstrated that FGFR and VEGFR were expressed on the surface of esophageal tumor cells (Fig. 4). These results suggest that FGFR and VEGFR are upregulated in the tumor cells and tissues of patients with esophageal cancer.

Efficacy of CECT-CNFV in the early diagnosis of patients with suspected esophageal cancer. The affinity of BisFV for FGFR and VEGFR was evaluated. As depicted in Figs. 5 and 6, Chitosan- Fe_3O_4 -encapsulated BisFV was able to bind FGFR and VEGFR, as determined by ELISA. The dose of nanoparticles that achieved optimum targeting efficiency was identified as 25 mg/kg (Table II). Subsequent analysis of patient clinical outcomes showed that 120 patients

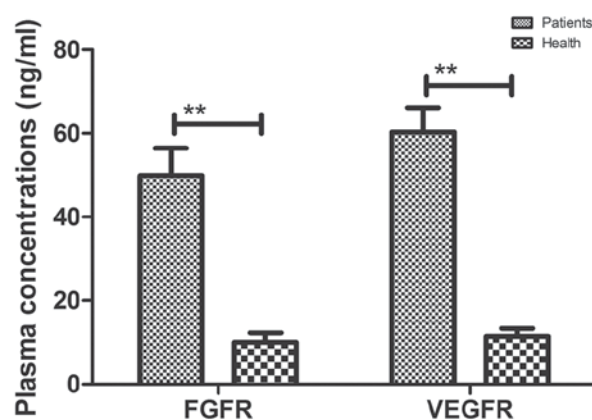


Figure 2. Comparison of the plasma concentrations of FGFR and VEGFR between esophageal cancer patients and healthy volunteers. A Student's t test revealed a significant effect. ** $P < 0.01$ vs. health. FGFR, fibroblast growth factor receptor; VEGFR, vascular endothelial growth factor receptor.

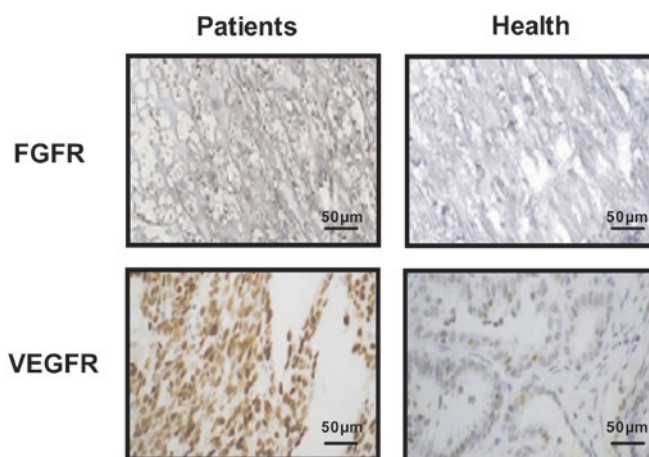


Figure 3. Expression levels of FGFR and VEGFR in the esophageal tumor tissues of cancer patients determined by immunohistochemistry. FGFR, fibroblast growth factor receptor; VEGFR, vascular endothelial growth factor receptor. Magnification, x40.

(37.50%) were diagnosed as tumor-free and 200 patients (62.50%) were confirmed to have esophageal cancer after diagnosis with CECT-CNFV. By contrast, the CECT method

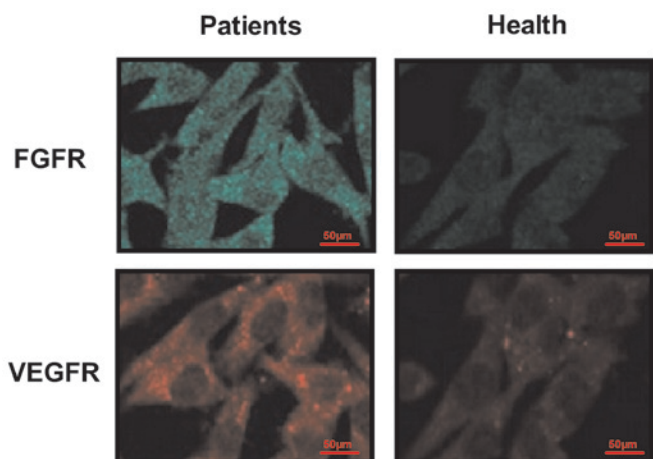


Figure 4. Immunofluorescence assay of green fluorescence-labeled FGFR and red fluorescence-labeled VEGFR in the esophageal tumor tissues of cancer patients. FGFR, fibroblast growth factor receptor; VEGFR, vascular endothelial growth factor receptor. Magnification, x100. Scale bar, 50 μ m.

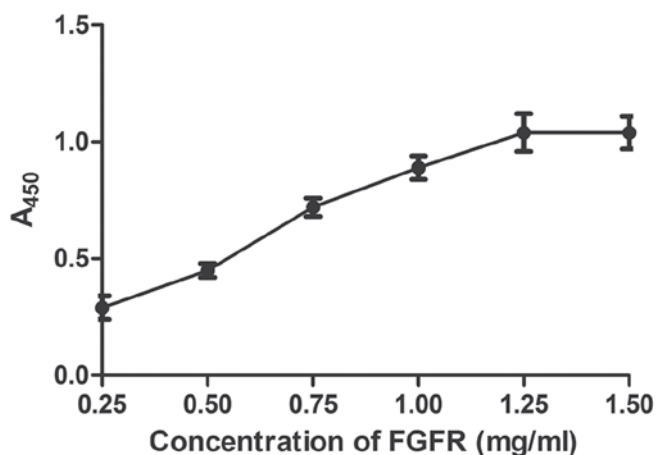


Figure 5. Affinity of bispecific antibody for FGFR determined by ELISA. FGFR, fibroblast growth factor receptor.

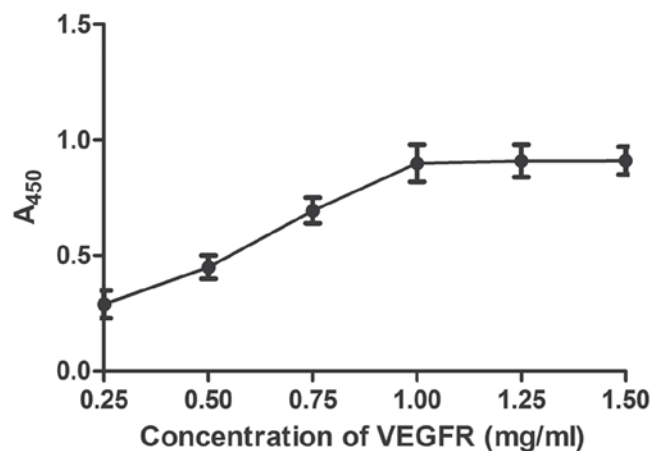


Figure 6. Affinity of bispecific antibody for VEGFR determined by ELISA. VEGFR, vascular endothelial growth factor receptor.

only diagnosed 45 patients (14.06%) with esophageal cancer Fig. 7). These outcomes demonstrated that CECT-CNFV

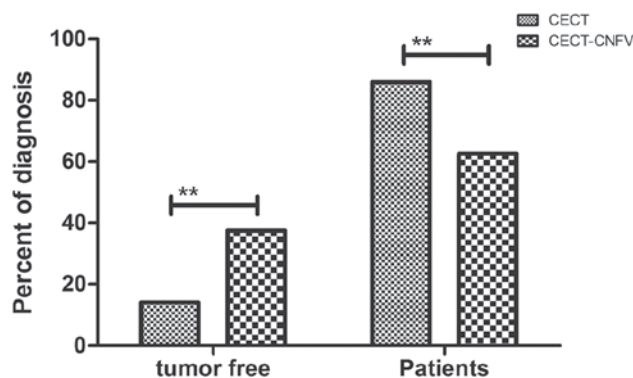


Figure 7. Comparison of the confirmed diagnosis rate determined by CECT-CNFV and CECT. A Student's t test revealed a significant effect. ** $P < 0.01$ CECT-CNFV vs. CECT. CECT, contrast-enhanced computed tomography; CECT-CNFV, CECT combined with Chitosan- Fe_3O_4 nanoparticles targeting fibroblast growth factor receptor and vascular endothelial growth factor receptor.

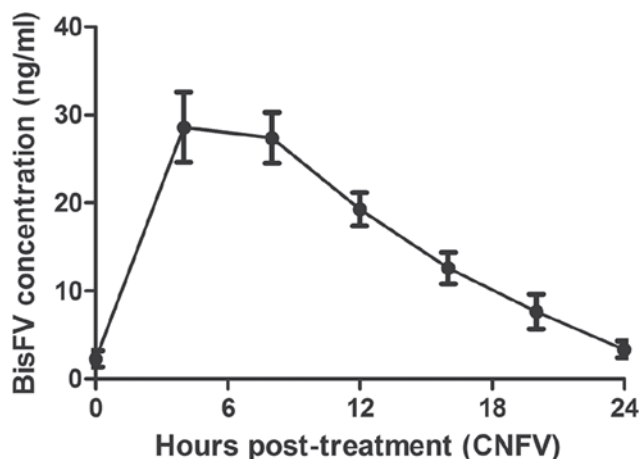


Figure 8. Metabolism of BisFV in contrast agent nanoparticles in the serum of patients with esophageal cancer following CECT-CNFV. BisFV, bispecific antibody against fibroblast growth factor receptor and vascular endothelial growth factor receptor; CECT-CNFV, contrast-enhanced computed tomography combined with Chitosan- Fe_3O_4 nanoparticles targeting fibroblast growth factor receptor and vascular endothelial growth factor receptor.

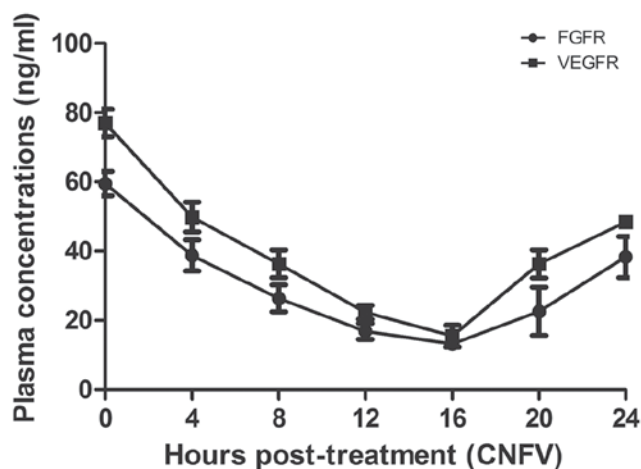


Figure 9. Plasma concentration levels of FGFR and VEGFR in the serum of patients with esophageal cancer following CECT-CNFV. FGFR, fibroblast growth factor receptor; VEGFR, vascular endothelial growth factor receptor; CECT-CNFV, contrast-enhanced computed tomography combined with Chitosan- Fe_3O_4 nanoparticles targeting FGFR and VEGFR.

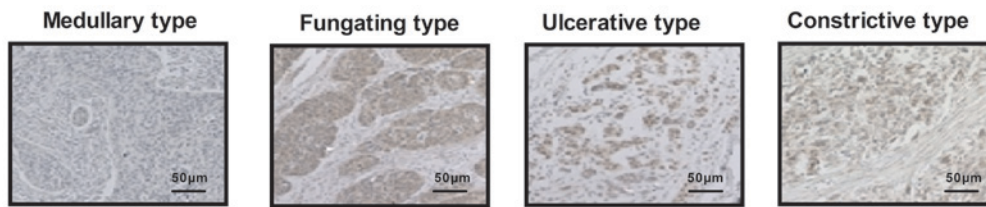


Figure 10. Histological analysis of esophageal cancer types in patients diagnosed by contrast-enhanced computed tomography combined with Chitosan-Fe₃O₄ nanoparticles targeting fibroblast growth factor receptor and vascular endothelial growth factor receptor. Magnification, x40.

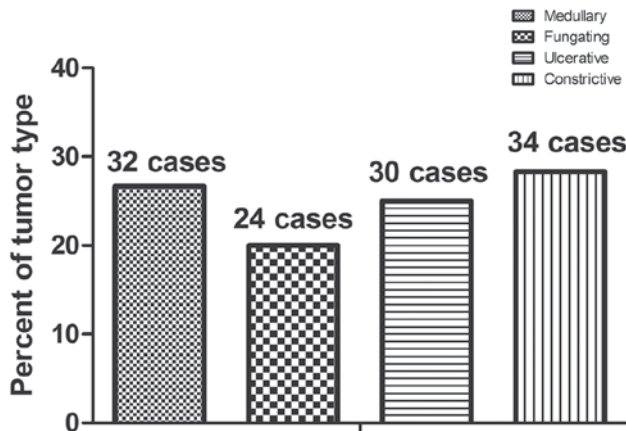


Figure 11. Incidence rates of esophageal cancer types in patients diagnosed by contrast-enhanced computed tomography combined with Chitosan-Fe₃O₄ nanoparticles targeting fibroblast growth factor receptor and vascular endothelial growth factor receptor.

presented significantly higher diagnostic efficacy compared with CECT ($P < 0.01$).

Pharmacodynamics of CNFV in the plasma of patients with suspected esophageal cancer. The pharmacodynamics of BisFV was assessed in the plasma of patients with suspected esophageal cancer. Results indicated that the plasma concentration of BisFV was increased and metabolized within 24 h using liquid chromatography-tandem mass spectrometry (Fig. 8). Patients that underwent CECT-CNFV exhibited reduced plasma concentrations of FGFR and VRGFR, both of which reached a minimum at 16 h post-treatment compared with the plasma concentrations prior to diagnosis (Fig. 9).

Accuracy of CECT-CNFV in the diagnosis of esophageal cancer. Histopathological analysis was performed to confirm that CECT-CNFV had successfully diagnosed esophageal cancer. The different types of early-stage esophageal cancer in patients, namely medullary, fungating, ulcerative and constrictive, were identified by immunohistochemistry (Fig. 10). A total of 120 cases of esophageal cancer were identified by immunohistochemistry, and the incidence rates of medullary, fungating, ulcerative and constrictive type esophageal cancer were 26.67% (32 cases), 20.00% (24 cases), 25.00% (30 cases) and 28.33% (34 cases), respectively (Fig. 11). As CECT-CNFV also identified 120 cases of esophageal cancer, these data suggest that CECT-CNFV may be a useful clinical method for the diagnosis of early-stage esophageal cancer.

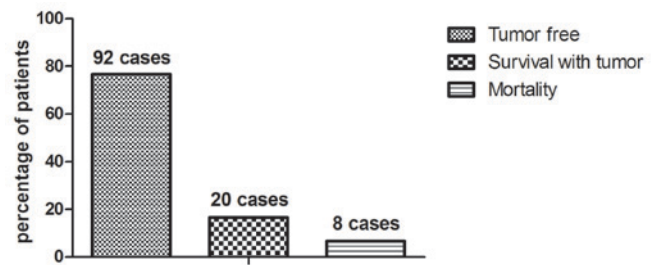


Figure 12. Rates of tumor free survival, survival with tumor and mortality in patients diagnosed by contrast-enhanced computed tomography combined with Chitosan-Fe₃O₄ nanoparticles targeting fibroblast growth factor receptor and vascular endothelial growth factor receptor.

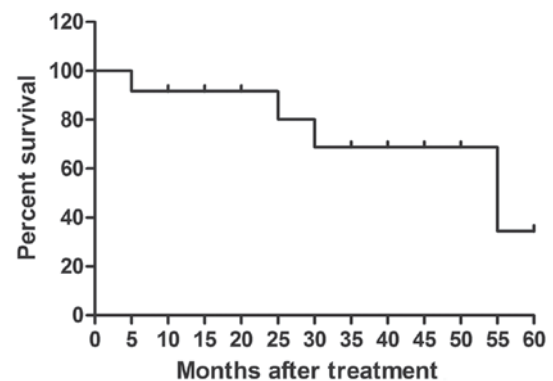


Figure 13. Median overall survival of patients with early-stage esophageal cancer diagnosed by contrast-enhanced computed tomography combined with Chitosan-Fe₃O₄ nanoparticles targeting fibroblast growth factor receptor and vascular endothelial growth factor receptor. Kaplan-Meier analysis was used to estimate the survival rate of patients during a 60-month long-term observation.

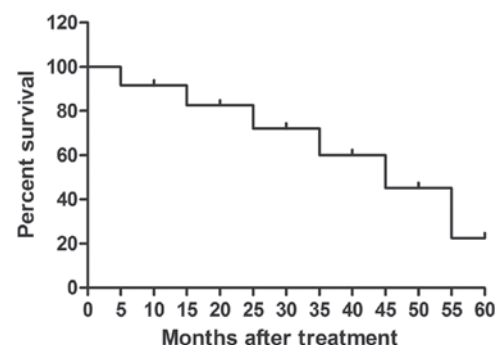


Figure 14. Median progression-free survival of patients with early-stage esophageal cancer diagnosed by contrast-enhanced computed tomography combined with Chitosan-Fe₃O₄ nanoparticles targeting fibroblast growth factor receptor and vascular endothelial growth factor receptor. Kaplan-Meier analysis was used to estimate the survival rate of patients during a 60-month long-term observation.

Survival rate of patients with esophageal cancer. Patients diagnosed with early-stage esophageal cancer received different treatments to inhibit or eradicate tumor growth (Table III). The overall survival rate of patients with esophageal cancer following diagnosis with CECT-CNFV was subsequently evaluated. At a 60-month follow-up, 92 patients (76.67%) had survived and were tumor-free, and 20 patients (16.66%) had survived with tumors. A total of 8 patients (6.67%) did not survive (Fig. 12). The median overall survival rate was 55.2 months (Fig. 13) and median progression-free survival rate was 44.6 months (Fig. 14). These data suggest that patients with early-stage esophageal cancer diagnosed by CECT-CNFV and administered with anti-cancer treatments present with longer survival rates.

Discussion

Early diagnosis of cancer is a significant challenge in the clinical treatment of human cancer (35,36). In recent years, contrast-enhanced ultrasound, CT and fluorodeoxyglucose-positron emission tomography have been widely used in the diagnosis of human cancers (37). In particular, CECT is the most widely used method in the diagnosis of human tumors (38,39). However, the accuracy and sensitivity of CECT is insufficient in the clinical detection of early-stage tumors (40,41). In the present study, a target nano-scale contrast agent combined with CECT was used to improve the accuracy and sensitivity of CECT in the diagnosis of patients with suspected early-stage esophageal cancer. The target nano-scale contrast agent was Chitosan-Fe₃O₄ nanoparticles encapsulated by BisFV, which may bind to esophageal cancer cells. The results indicated that CECT-CNFV not only improved the resolution ratio of images captured by CECT, but also increased the accuracy and sensitivity of CECT in the diagnosis of patients with suspected early-stage esophageal cancer.

Theoretically, a nano-scale contrast agent may improve *in vivo* tumor imaging made by ultrasound, CT and magnetic resonance imaging (42-44). Kim *et al* (42) demonstrated that ultrasound enhanced-contrast agents, which may go preferentially to the target tumor tissue and amplify the ultrasound imaging signal *in vivo*, improved the detection limit of ultrasound imaging. Furthermore, Ding *et al* (43) demonstrated that targeted Fe-filled carbon nanotube as a multifunctional contrast agent improved the resolution ratio of magnetic resonance imaging of tumors in living mice. These reports indicate that nano-scale contrast agents may be useful for detecting tumor masses in early-stage cancer.

In the present study, a novel nano-scale contrast agent composed of Chitosan-Fe₃O₄ nanoparticles encapsulated by BisFV was introduced to evaluate the efficacy of CECT-CNFV in the diagnosis of patients with suspected esophageal cancer. Barium sulfate and iodinated contrast media are frequently used for angiography studies and in the detection of tumors in the digestive system (45,46). Various kinds of electro-positive iron and iron oxide nanoparticles have been used as contrast media in combination with ultrasound, CT and magnetic resonance imaging for the clinical diagnosis of human cancers (47,48). In addition, targeted contrast agents are considered to enhance optical coherence tomography and

improve the accuracy of CT in the diagnosis of tumor tissue masses (49). However, although contrast media improve the accuracy of CT to a certain degree, their sensitivity has not been improved in previous studies (21,50). The present results indicated that CECT-CNFV was efficient in the targeting of FGFR and VEGFR, and improved the accuracy and sensitivity of CT in the diagnosis of early-stage esophageal cancer. Notably, long-term follow-up investigations suggested that patients diagnosed by CECT-CNFV at early-stage presented with higher median overall survival and median progression-free survival rates compared with the mean survival rate of patients with esophageal cancer in previous reports (51).

In conclusion, the present study investigated the efficacy of CECT-CNFV in the diagnosis of suspected early-stage esophageal cancer. Chitosan-Fe₃O₄ nanoparticles encapsulated by BisFV not only improved the image resolution generated by CT, but also enhanced the accuracy and sensitivity of CT in the diagnosis of early-stage esophageal cancer. These outcomes indicate that CECT-CNFV may be an efficient clinical method for diagnosing patients with suspected esophageal cancer at an early-stage. Thus, CECT-CNFV may be a reliable and sensitive assessment method in the clinical diagnosis of cancer patients.

Competing interests

The authors declare that they have no competing interests.

References

- Findlay JM, Middleton MR and Tomlinson I: A systematic review and meta-analysis of somatic and germline DNA sequence biomarkers of esophageal cancer survival, therapy response and stage. *Ann Oncol* 26: 624-644, 2015.
- Malik MA, Zargar SA and Mittal B: Role of NQO1 609C>T and NQO2-3423G>A gene polymorphisms in esophageal cancer risk in Kashmir valley and meta analysis. *Mol Biol Rep* 39: 9095-9104, 2012.
- Chen M, Cai E, Huang J, Yu P and Li K: Prognostic value of vascular endothelial growth factor expression in patients with esophageal cancer: A systematic review and meta-analysis. *Cancer Epidemiol Biomarkers Prev* 21: 1126-1134, 2012.
- Jacobs M, Macefield RC, Blazeby JM, Korfage IJ, van Berge Henegouwen MI, de Haes HC, Smets EM and Sprangers MA: Systematic review reveals limitations of studies evaluating health-related quality of life after potentially curative treatment for esophageal cancer. *Qual Life Res* 22: 1787-1803, 2013.
- Samson P, Robinson C, Bradley J, Lockhart AC, Puri V, Broderick S, Kreisel D, Krupnick AS, Patterson GA, Meyers B and Crabtree T: Neoadjuvant chemotherapy versus chemoradiation prior to esophagectomy: Impact on rate of complete pathologic response and survival in esophageal cancer patients. *J Thorac Oncol* 11: 2227-2237, 2016.
- Liao J, Liu R, Shi YJ, Yin LH and Pu YP: Exosome-shuttling microRNA-21 promotes cell migration and invasion-targeting PDCD4 in esophageal cancer. *Int J Oncol* 48: 2567-2579, 2016.
- Guo J, Yu X, Gu J, Lin Z, Zhao G, Xu F, Lu C and Ge D: Regulation of CXCR4/AKT-signaling-induced cell invasion and tumor metastasis by RhoA, Rac-1, and Cdc42 in human esophageal cancer. *Tumour Biol* 37: 6371-6378, 2016.
- Pan Z, Mao W, Bao Y, Zhang M, Su X and Xu X: The long noncoding RNA CASC9 regulates migration and invasion in esophageal cancer. *Cancer Med* 5: 2442-2447, 2016.
- Shi H, Shi D, Wu Y, Shen Q and Li J: Qigesan inhibits migration and invasion of esophageal cancer cells via inducing connexin expression and enhancing gap junction function. *Cancer Lett* 380: 184-190, 2016.
- Schiefer AI, Schoppmann SF and Birner P: Lymphovascular invasion of tumor cells in lymph node metastases has a negative impact on survival in esophageal cancer. *Surgery* 160: 331-340, 2016.

11. Yokota T, Igaki H, Kato K, Tsubosa Y, Mizusawa J, Katayama H, Nakamura K, Fukuda H and Kitagawa Y: Accuracy of preoperative diagnosis of lymph node metastasis for thoracic esophageal cancer patients from JCOG9907 trial. *Int J Clin Oncol* 21: 283-288, 2016.
12. Visser E, Leeftink AG, van Rossum PS, Siesling S, van Hillegersberg R and Ruurda JP: Waiting time from diagnosis to treatment has no impact on survival in patients with esophageal cancer. *Ann Surg Oncol* 23: 2679-2689, 2016.
13. Ishigaki M, Maeda Y, Taketani A, Andriana BB, Ishihara R, Wongravee K, Ozaki Y and Sato H: Diagnosis of early-stage esophageal cancer by Raman spectroscopy and chemometric techniques. *Analyst* 141: 1027-1033, 2016.
14. Kawada S and Imai Y: Diagnosis of esophageal cancer and metastatic lymph node using CT and MRI. *Nihon Rinsho* 69 (Suppl 6): S174-S181, 2011 (In Japanese).
15. Freling N, Roele E, Schaefer-Prokop C and Fokkens W: Prediction of deep neck abscesses by contrast-enhanced computerized tomography in 76 clinically suspect consecutive patients. *Laryngoscope* 119: 1745-1752, 2009.
16. Yang DH, Min JJ, Jeong YY, Ahn JS, Kim YK, Cho SH, Chung IJ, Bom HS, Kim HJ and Lee JJ: The combined evaluation of interim contrast-enhanced computerized tomography (CT) and FDG-PET/CT predicts the clinical outcomes and may impact on the therapeutic plans in patients with aggressive non-Hodgkin's lymphoma. *Ann Hematol* 88: 425-432, 2009.
17. Kanat O, O'Neil B and Shahda S: Targeted therapy for advanced gastric cancer: A review of current status and future prospects. *World J Gastrointestinal Oncol* 7: 401-410, 2015.
18. Kakimoto N, Chindasombataroen J, Tomita S, Shimamoto H, Uchiyama Y, Hasegawa Y, Kishino M, Murakami S and Furukawa S: Contrast-enhanced multidetector computerized tomography for odontogenic cysts and cystic-appearing tumors of the jaws: Is it useful? *Oral Surg Oral Med Oral Pathol Oral Radiol* 115: 104-113, 2013.
19. Mazzei MA, Guerrini S, Mazzei FG, Cioffi Squitieri N, Notaro D, de Donato G, Galzerano G, Sacco P, Setacci F, Volterrani L and Setacci C: Follow-up of endovascular aortic aneurysm repair: Preliminary validation of digital tomosynthesis and contrast enhanced ultrasound in detection of medium- to long-term complications. *World J Radiol* 8: 530-536, 2016.
20. Schalk S, Demi L, Bouhouch N, Kuenen MPJ, Postema AW, de la Rosette JJMCH, Wijkstra H, Tjalkens TJ and Mischi M: Contrast-enhanced Ultrasound Angiogenesis Imaging by mutual information analysis for prostate cancer localization. *IEEE Trans Biomed Eng* 64: 661-670, 2017.
21. Shi H, Wang Z, Huang C, Gu X, Jia T, Zhang A, Wu Z, Zhu L, Luo X, Zhao X, *et al*: A functional ct contrast agent for in vivo imaging of tumor hypoxia. *Small* 12: 3995-4006, 2016.
22. Wheatley MA, Forsberg F, Dube N, Patel M and Oeffinger BE: Surfactant-stabilized contrast agent on the nanoscale for diagnostic ultrasound imaging. *Ultrasound Med Biol* 32: 83-93, 2006.
23. Fons P, Gueguen-Dorbes G, Herault JP, Geronimi F, Tuyaret J, Frédérique D, Schaeffer P, Volle-Challier C, Herbert JM and Bono F: Tumor vasculature is regulated by FGF/FGFR signaling-mediated angiogenesis and bone marrow-derived cell recruitment: This mechanism is inhibited by SSR128129E, the first allosteric antagonist of FGFRs. *J Cell Physiol* 230: 43-51, 2015.
24. Valesky M, Spang AJ, Fisher GW, Farkas DL and Becker D: Noninvasive dynamic fluorescence imaging of human melanomas reveals that targeted inhibition of bFGF or FGFR-1 in melanoma cells blocks tumor growth by apoptosis. *Mol Med* 8: 103-112, 2002.
25. Takahashi O, Komaki R, Smith PD, Jürgensmeier JM, Ryan A, Bekele BN, Wistuba II, Jacoby JJ, Korshunova MV, Biernacka A, *et al*: Combined MEK and VEGFR inhibition in orthotopic human lung cancer models results in enhanced inhibition of tumor angiogenesis, growth, and metastasis. *Clin Cancer Res* 18: 1641-1654, 2012.
26. Bozec A, Formento P, Lassalle S, Lippens C, Hofman P and Milano G: Dual inhibition of EGFR and VEGFR pathways in combination with irradiation: Antitumour supra-additive effects on human head and neck cancer xenografts. *Br J Cancer* 97: 65-72, 2007.
27. Yang Z, Lu A, Wong BC, Chen X, Bian Z, Zhao Z, Huang W, Zhang G, Chen H and Xu M: Effect of liposomes on the absorption of water-soluble active pharmaceutical ingredients via oral administration. *Curr Pharm Des* 19: 6647-6654, 2013.
28. Chen CL, Hu GY, Mei Q, Qiu H, Long GX and Hu GQ: Epidermal growth factor receptor-targeted ultra-small superparamagnetic iron oxide particles for magnetic resonance molecular imaging of lung cancer cells in vitro. *Chin Med J (Engl)* 125: 2322-2328, 2012.
29. Granja RH, Salerno AG, de Lima AC, Montalvo C, Reche KV, Giannotti FM and Wanschel AC: Liquid chromatography/tandem mass spectrometry method to determine boldenone in bovine liver tissues. *J AOAC Int* 97: 1476-1480, 2014.
30. Ghantous Y, Naddaf R, Barak M, Abd-Elraziq M and Abu Eln-Naaj I: The role of fine needle aspiration in the diagnosis of parotid gland tumors: Correlation with preoperative computerized tomography tumor size. *J Craniofac Surg* 27: e192-e196, 2016.
31. Angelov KG, Vasileva MB, Grozdev KS, Sokolov MB and Todorov G: Clinical and pathological characteristics, and prognostic factors for gastric cancer survival in 155 patients in Bulgaria. *Hepatogastroenterology* 61: 2421-2424, 2014.
32. Sawasdikosol S: Detecting tyrosine-phosphorylated proteins by Western blot analysis. *Curr Protoc Immunol Chapter 11: Unit 11 13 11-11*, 2010.
33. Dirani M, Nasreddine W, Abdulla F and Beydoun A: Seizure control and improvement of neurological dysfunction in Lafora disease with perampanel. *Epilepsy Behav Case Rep* 2: 164-166, 2014.
34. Kargahi N, Razavi SM, Deyhimi P and Homayouni S: Comparative evaluation of eosinophils in normal mucosa, dysplastic mucosa and oral squamous cell carcinoma with hematoxylin-eosin, Congo red, and EMRI immunohistochemical staining techniques. *Electron Physician* 7: 1019-1026, 2015.
35. Wei R, Guo B and Tan ZM: Application of tumor markers detection in early diagnosis of oral maxillofacial-head and neck carcinomas. *Zhonghua Kou Qiang Yi Xue Za Zhi* 43: 143-145, 2008 (In Chinese).
36. Neven P, Brouckaert O, Van Belle V, Vanden Bempt I, Hendrickx W, Cho H, Deraedt K, Van Calster B, Van Huffel S, Moerman P, *et al*: In early-stage breast cancer, the estrogen receptor interacts with correlation between human epidermal growth factor receptor 2 status and age at diagnosis, tumor grade, and lymph node involvement. *J Clin Oncol* 26: 1768-1771, 2008.
37. Ebell MH, Culp MB and Radke TJ: A systematic review of symptoms for the diagnosis of ovarian cancer. *Am J Prev Med* 50: 384-394, 2016.
38. de Moura PM, Hallac R, Kane A and Seaward J: Improving the evaluation of alveolar bone grafts with cone beam computerized tomography. *Cleft Palate Craniofac J* 53: 57-63, 2016.
39. Fang L, Jingjing L, Ying S, Lan M, Tao W and Nan J: Computerized tomography-guided sphenopalatine ganglion pulsed radiofrequency treatment in 16 patients with refractory cluster headaches: Twelve- to 30-month follow-up evaluations. *Cephalalgia* 36: 106-112, 2016.
40. Benharroch D, Shvarts S, Jotkowitz A and Shelef I: Computerized tomography scanning and magnetic resonance imaging will terminate the era of the autopsy-a hypothesis. *J Cancer* 7: 115-120, 2016.
41. Lambert S, Al-Hadithy N, Sewell MD, Hertel R, Südkamp N, Noser H and Kamer L: Computerized tomography based 3D modeling of the clavicle. *J Orthop Res* 34: 1216-1223, 2016.
42. Kim M, Lee JH, Kim SE, Kang SS and Tae G: Nanosized ultrasound enhanced-contrast agent for in vivo tumor imaging via intravenous injection. *ACS Appl Mater Interfaces* 8: 8409-8418, 2016.
43. Ding W, Lou C, Qiu J, Zhao Z, Zhou Q, Liang M, Ji Z, Yang S and Xing D: Targeted Fe-filled carbon nanotube as a multifunctional contrast agent for thermoacoustic and magnetic resonance imaging of tumor in living mice. *Nanomedicine* 12: 235-244, 2016.
44. Wang W, Li J, Liu R, Zhang A and Yuan Z: Size effect of Au/PAMAM contrast agent on CT imaging of reticuloendothelial system and tumor tissue. *Nanoscale Res Lett* 11: 429, 2016.
45. Konduru N, Keller J, Ma-Hock L, Gröters S, Landsiedel R, Donaghey TC, Brain JD, Wohlleben W and Molina RM: Biokinetics and effects of barium sulfate nanoparticles. *Part Fibre Toxicol* 11: 55, 2014.
46. Liss P, Hansell P, Fasching A and Palm F: Iodinated contrast media inhibit oxygen consumption in freshly isolated proximal tubular cells from elderly humans and diabetic rats: Influence of nitric oxide. *Ups J Med Sci* 121: 12-16, 2016.

47. Mishra SK, Kumar BS, Khushu S, Tripathi RP and Gangenahalli G: Increased transverse relaxivity in ultrasmall superparamagnetic iron oxide nanoparticles used as MRI contrast agent for biomedical imaging. *Contrast Media Mol Imaging* 11: 350-361, 2016.
48. Kitoh Y: 5. Inspection of hepatocellular carcinoma 3-contrast for the diagnosis of hepatocellular carcinoma: Techniques of image contrast and the choice of MR contrast agent. *Nihon Hoshasen Gijutsu Gakkai Zasshi* 72: 441-451, 2016 (In Japanese).
49. Zhang J, Liu J, Wang LM, Li ZY and Yuan Z: Retroreflective-type Janus microspheres as a novel contrast agent for enhanced optical coherence tomography. *J Biophotonics* 10: 878-886, 2017.
50. D'Hollander A, Mathieu E, Jans H, Vande Velde G, Stakenborg T, Van Dorpe P, Himmelreich U and Lagae L: Development of nanostars as a biocompatible tumor contrast agent: Toward in vivo SERS imaging. *Int J Nanomedicine* 11: 3703-3714, 2016.
51. Huang YM, Wang CH, Huang JS, Tsai CS, Yeh KY, Lan YJ, Wu TH, Chang PH, Chang YS and Lai CH: Treatment-associated severe thrombocytopenia affects survival rate in esophageal cancer patients undergoing concurrent chemoradiotherapy. *Indian J Cancer* 52: 454-460, 2015.



This work is licensed under a Creative Commons Attribution-NonCommercial-NoDerivatives 4.0 International (CC BY-NC-ND 4.0) License.